Journal of Luminescence 183 (2017) 322–333

Contents lists available at ScienceDirect

Journal of Luminescence

journal homepage: www.elsevier.com/locate/jlumin

Delayed chlorophyll a fluorescence, MR 820, and gas exchange changes in perennial ryegrass under salt stress

P. Dąbrowski [a,*], M.H. Kalaji [b,c], A.H. Baczewska [d], B. Pawluśkiewicz [a], G. Mastalerczuk [e], B. Borawska-Jarmułowicz [e], M. Paunov [f], V. Goltsev [f]

[a] *Department of Environmental Improvement, Warsaw University of Life Sciences-SGGW, 159 Nowoursynowska St., 02-776 Warsaw, Poland*
[b] *Department of Plant Physiology, Warsaw University of Life Sciences-SGGW, 159 Nowoursynowska St., 02-776 Warsaw, Poland*
[c] *SI TECHNOLOGY Sp. z o. o., Górczewska 226C/26, 01-460 Warsaw, Poland*
[d] *Polish Academy of Sciences Botanical Garden-Center for Biological Diversity Conservation in Powsin, 2 Prawdziwka St., 02-973 Warsaw, Poland*
[e] *Department of Agronomy, Warsaw University of Life Sciences-SGGW, 159 Nowoursynowska St., 02-776 Warsaw, Poland*
[f] *Department Biophysics and Radiobiology, St. Kl. Ohridski Sofia University, 8 Dragan Tsankov Blvd., 1164 Sofia, Bulgaria*

ARTICLE INFO

Article history:
Received 8 September 2016
Received in revised form
25 October 2016
Accepted 10 November 2016
Available online 21 November 2016

Keywords:
Lawn grasses
Plant stress
Photosynthesis

ABSTRACT

Perennial ryegrass (*Lolium perenne* L.) is one of the more popular grass species in Europe. It is commonly used for starting lawns in urban areas, where plant growth is limited by many environmental conditions. The contamination of soils by salt is one of the major problems in urban green areas, as well as in natural areas. The basic aim of this study is to provide a detailed *in vivo* analysis of the changes in the delayed chlorophyll fluorescence and MR 820 signals (induced by salt stress) of two lawn varieties of perennial ryegrass, and to find out if there are correlations between these parameters and gas exchange. Two lawn varieties of *Lolium perenne* L. were used: Nira and Roadrunner. Salinization was performed at 8 weeks after sowing by adding NaCl in water solution (0, 0.15, and 0.30 M). There were 8 terms of measurement: 0 h, 24 h, 48 h, 96 h, 144 h, 192 h, 240 h, and 288 h after salinization. Our results showed that delayed fluorescence is a tool that can bring completely new opportunities for detecting stress in plants caused by salt. Our work allowed us to identify various limitation patterns in the photosynthetic efficiency of perennial ryegrass lawn varieties grown under salt stress conditions. Significant differences between the two tested varieties in response to salt stress were confirmed.

1. Introduction

Urban green areas have various functions important to the quality of human health. Well-kept lawns enhance the aesthetic value of the entire city and are involved in phytoremediation, leading to an improvement in the quality of the air and soil. Perennial ryegrass (*Lolium perenne* L.) is one of the most popular grass species in Europe. It is widely used as a forage crop, as an alternative and renewable bioenergy source, and for starting lawns in urban areas [1,2].

Salt stress is one of the major environmental conditions in urban areas that influences the growth and development of plants. The NaCl used for de-icing slippery roads in the winter is now recognized as one of the major causes of soil contamination [3]. Many plant species used on lawns near roads are very sensitive to the high salt concentrations associated with a decreased photosynthesis rate. In the past, gas exchange was the most popular tool for diagnosing plant response to stress. Nowadays, chlorophyll *a* fluorescence measurements (ChFl) are more and more popular as a likely technique [4–7]. It allows for the measurement of plant vitality under unfavorable environmental conditions through the analysis of fluorescence transients. The parameters measured are in close correlation with the functioning of photosystem II (PS II). Stress applied to green plants that directly or indirectly affects the photosynthetic metabolism is likely to change the yield of chlorophyll fluorescence. Analyses of fluorescence quenching provide information on the energy absorption, utilization, dissipation, and the electron transport in PSII [8–10]. This makes it possible to evaluate a plant's photosynthetic performance and the extent of its tolerance to salt stress [11,12]. Light absorbed by chlorophyll molecules for photochemical reactions can be converted back into

---

[*] Corresponding author.
E-mail addresses: piotr_dabrowski@sggw.pl,
bogumila_pawluskiewicz@sggw.pl (P. Dąbrowski), hazem@kalaji.pl (M.H. Kalaji),
a.baczewska@obpan.pl (A.H. Baczewska),
grazyna_mastalerczuk@sggw.pl (G. Mastalerczuk),
barbara_borawska_jarmulowicz@sggw.pl (B. Borawska-Jarmułowicz),
goltsev@biofac.uni-sofia.bg (V. Goltsev).

http://dx.doi.org/10.1016/j.jlumin.2016.11.031

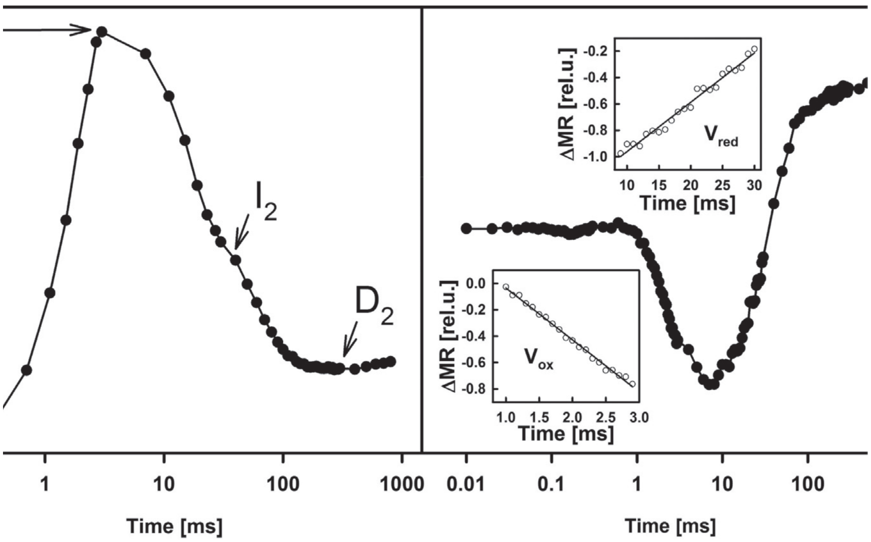

Fig. 1. A – Typical transient of the delayed fluorescence (DF) intensity recorded in the microsecond dark decay interval (from 20 to 90 μs) during the first induction. The DF signal is measured in dark-adapted leaves of control ryegrass plants (variety Nira). The main specific local maxima (I_1 and I_2) and minimum (D_2) are indicated with arrows. B – Typical induction curve of the reflection of modulated light at 820 nm (MR820) recorded in dark adapted leaves of control plants Nira variety. The inserts show the derivation of the apparent rates of oxidation (V_{ox}) and reduction (V_{red}) of the PSI reaction center (P700). V_{ox} is calculated as the slope of the linear fit of the MR820 signal decrease (1–2.9 ms) and V_{red} – of the MR820 rise between 9 and 30 ms.

light as prompt fluorescent (PF) or delayed fluorescent (DF). Both are emitted from the PSII antenna complex, but there are fundamental differences between them.

Based on results obtained during ChFl measurements, it is known that salinity stress influence on the electron transport from the RCs to the plastoquinone pool [13]. The OEC (Oxygen-evolving complex) was identified as one of the most sensitive components in the photosynthetic electron transport chain. Its reduced performance is usually caused by an electron transport disorder. Modifications is also noted in ChFl parameters and PSII functioning. Under high salinity conditions, electron trapping in PSII reaction center becomes less efficient due to the dissociation of LHCII and PSII [14]. A decrease in maximum quantum yield of PSII and an increase in non-photochemical quenching have been recorded by measuring the ChFl. Moreover, the following parameters were reduced during salinity stress: PSII efficiency in light, electron transport chain efficiency, and the efficiency of PSII open reaction centers in light [15,16]. The damage caused by salinity stress was more prominent at the donor side rather than the acceptor side of PSII, and this damage was fully reversible at the acceptor side of PSII, while recovery of the donor side was less pronounced [17]. The osmotic and ionic effects of salinity stress have also been differentiated using ChlF measurements [18].

A single molecule is sufficient for the generation of a PF signal. The DF depends on system interactions [19], which makes DF a potential indicator of photosynthesis efficiency and plant stress [20,21]. DF emission occurs for a short time after prompt fluorescence decay. DF emitted in micro- and millisecond time ranges has been thought to reflect the recombination, in the dark, of the reduced electron acceptor Q_A^- and the oxidized secondary electron donor Z^+ of PSII. These oxidized electron donors are formed after light-induced charge separation. In a matter of seconds DF is associated with the recombination of S_2 or S_3 states of the oxygen-evolving complex (OEC) with Q_A^- or Q_B^-.

DF emission displays multiple phases over the emission time span [22]. These phases correlated to individual elements of the electron transport chain. The exact mechanism for the final DF emission is not yet fully understood. There are different theory [23]: the electron-hole recombination theory [24], the triplet fusion theory [25], and the charge-recombination theory [26]. The charge-recombination theory is more common [24]. The exact mechanism, however, does not alter the fact that the exited electrons come from different stages of the electron transport chain. A variable that influences PSII functions may affect DF emission and thus can be potentially indicated by DF. There is less knowledge about the DF induction curve in comparison with the PF transients. The DF induction curve has several maxima and minima. Their number and amplitude, however, depend on the kinetic components of the DF being measured [27]. Moreover, the amplitudes and lifetimes of the ms DF during the induction period vary significantly [28]. There is no one nomenclature of the maxima, as well as no consensus about the number and interpretation of these maxima. In this work the maxima (denoted by I) and minima (labeled D) were numbered in sequence according to their position in the IC (I_1, I_2, D_2) according to Goltsev et al. [28].

The modulated reflection (MR) signal measured at 820 nm provides information about electron transport from the plastoquinone (PQ) and to the photosystem I (PS I) acceptors [29,30], thus indicating changes in the redox state of the PS I reaction centers (RC) and plastocyanin (PC). All redox reactions of the photosynthetic electron transport between PS II and PS I and all electron transfer reactions in the reaction centers (RC) of PS II (donor and acceptor side) are reversible. The accumulation of electrons in the electron transport chain between PS I and PS II leads back to electron transfer and charge recombination in PS II RC, resulting in the re-excitation of the RC and the repopulation, by fast energy transfer, of the excited chlorophyll state of PS II antennae [31].

In opinion of Goltsev et al. [12] simultaneous measurements of the PF, DF and MR820 are important for complete correlation of the information about influence of stress factor on the ETC. By virtue of this correlation, research is being conducted to demonstrate the importance of such simultaneous analysis, that can donate or accept electrons at specific locations in the electron transport chain [32]. There is in literature information about PF changes under salt stress. However, no data can be found in the literature on the simultaneous analysis of DF and MR820 where these inhibitors are used. The example of DF and MR820 curves were shown in Fig. 1.

There is a lack of work in the literature about the influence of salinity on perennial ryegrass lawn varieties. There is also no literature about delayed fluorescence and MR 820 signal changes caused by salinity in comparison with gas exchange. Therefore, the basic aim of this study was to conduct a detailed in vivo analysis of changes in delayed fluorescence and MR 820 kinetics induced by salt stress in two lawn varieties of perennial ryegrass in comparison with gas exchange parameters. In addition, we also tested whether the chlorophyll fluorescence data could be used to recognize the differences between the tested varieties.

2. Material and methods

2.1. Plants, growth conditions and experiment design

The experiment was conducted in the greenhouse at Warsaw University of Life Sciences (SGGW) under natural light for a period of day and night. The average temperature for day and night was 25/17 °C. Two lawn varieties of *Lolium perenne* L. were used for the experiment: Nira (Małopolska Hodowla Roślin, Poland) and Roadrunner (Turf Seed, Inc., USA). On 29 April 2014 seeds of both varieties were sown in pots (13 × 13 cm) filled with a mixed substrate containing sand (70%) and clay (30%). The seed dose was 0.42 g/pot. Salinization was started 8 weeks after sowing by adding a water solution of NaCl to each pot. 3 solutions were applied: 0 M NaCl (control), 0.15 M NaCl, and 0.30 M NaCl. The electrical conductance and moisture of the salinized substrate were measured by a Delta T-Device. The results from the soil properties chosen (soil moisture and electronic conductance) in each of the varieties are shown in Table 1.

The experiment was conducted in a spin–plot system. All of the measurements were carried out on flag leaves under uniform conditions and repeated 9 times. There were 8 terms of measurement: before and 24 h, 48 h, 96 h, 144 h, 192 h, 240 h and 288 h after the salt stress application. All measurements were made in a laboratory at 26 °C, with a 60% relative humidity and a photosynthetic photon flux rate of about 1000 μmol m^{-2} s^{-1}.

2.2. Delayed chlorophyll fluorescence and 820 mn light reflection measurements

Measurements were made on the adaxial surface of 9 leaves, after adapting to darkness for 30 min. For simultaneous record of the signals of DF and reflection of the a modulated light at 820 nm (MR) an M-PEA device (Multi-Function Plant Efficiency Analyzer, Hansatech, UK) was used with the following protocol: time duration of 1.0 s and actinic light illumination of 3000 μ mol m^{-2} s^{-1}. In the M-PEA instrument emitter the wavelength ranges were the following: 635 ± 10 nm for the actinic light LED (light-emitting diode); 820 ± 25 nm for the modulated light LED; 735 ± 15 nm for the far-red light LED.

For delayed fluorescence signal acquisition the plant sample is illuminated by modulated light, consisting a series of sequential light and dark periods in ratio 3:1. The duration of these periods rises stepwise during the induction. At the starting point of the measurement, after 300 µs illumination the dark interval lasts 100 µs, after 3 ms the durations of light and dark intervals becomes 10 times longer and then they are multiplied at 30th ms, 300th ms etc. DF is measured during the dark interval every 10 µs and the first point is recorded 20 µs after the light switch off. In the dark the DF signal decays poli-exponentially and to construct an induction curve of the microsecond DF component the signals recorded within interval from 20 to 90 µs are integrated. For the accurate determination of the kinetic characteristics of the DF decay curve the experimental points are fitted as poliexponential function:

$$DF = L_0 + \sum_i L_i \times exp^{-\frac{t}{\tau_i}},$$

where t is the time passed in dark, L_0 is the measured base DF level (characteristic of the device), L represents the amplitude and τ is the lifetime of i-th DF component. From the parameters of the fitted functions the amplitude (L_1) and the lifetime (τ_1) of the microsecond component are found.

The characteristic points (I_1, I_2 and D_2) of the DF induction curve were estimated. The I_1 point is the first maximum of the curve, the I_2 point is the second maximum, and the D_2 is the minimum of the curve. Based on their points, the two ratios were calculated: (I_1-D_2)/D_2 and I_1/I_2. The reflected MR signal was also measured at the same time as that of the DF. The ratio MR_t/MR_0, where MR_t indicates a modulated 820 nm reflection intensity at time t, with MR_0 being the value of the 820 nm reflection of the sample calculated at the onset of actinic illumination. The $MR_{min,}$ $MR_{max,}$ $_\Delta MR_{fast}$ and $_\Delta MR_{slow}$ were all calculated.

2.3. Gas exchange measurements

The photosynthetic rate in terms of net CO_2 assimilation (*An*), in addition to the transpiration rate (*E*), stomatal conductance (G_s) and the internal CO_2 concentration (C_i), were all measured on the leaves attached using a portable gas analyzer Lcpro+(ADC BioScientific Ltd, UK). This open-gas exchange system operated during measurement on a differential mode at a 150 mol s^{-1} flow rate of ambient air. The measurements were taken on 9 leaves in each treatment, and were taken after the stabilization of conditions in the chamber.

2.4. Statistical analysis

All experiments were carried out and repeated at least 9 times. The chlorophyll fluorescence parameters and gas exchange parameters were statistically analyzed both by the ANOVA model and by the Fischer's test (as a post hoc) at a 0.05 confidence level using the Statistica 10.0 program (Statsoft, Inc., Tulsa, OK, USA). The mathematical relationship between DF, the MR 820 signal, and CO_2 assimilation were estimated based on Pearson's correlation coefficient at a 0.05 confidence level.

3. Results

3.1. Delayed chlorophyll fluorescent induction curves and changes in light reflection at 820 nm (I820)

In this work attention was focused on the first recorded DF

Table 1
Chosen soil properties.

Variety	Control		0.15 M/L		0.30 M/L	
	Moisture [%]	Electrical conductance [mS m^{-1}]	Moisture [%]	Electrical conductance [mS m^{-1}]	Moisture [%]	Electrical conductance [mS m^{-1}]
Nira	27.5	237	29.4	624	27.4	850
Roadrunner	30.1	248	30.7	659	28.9	873

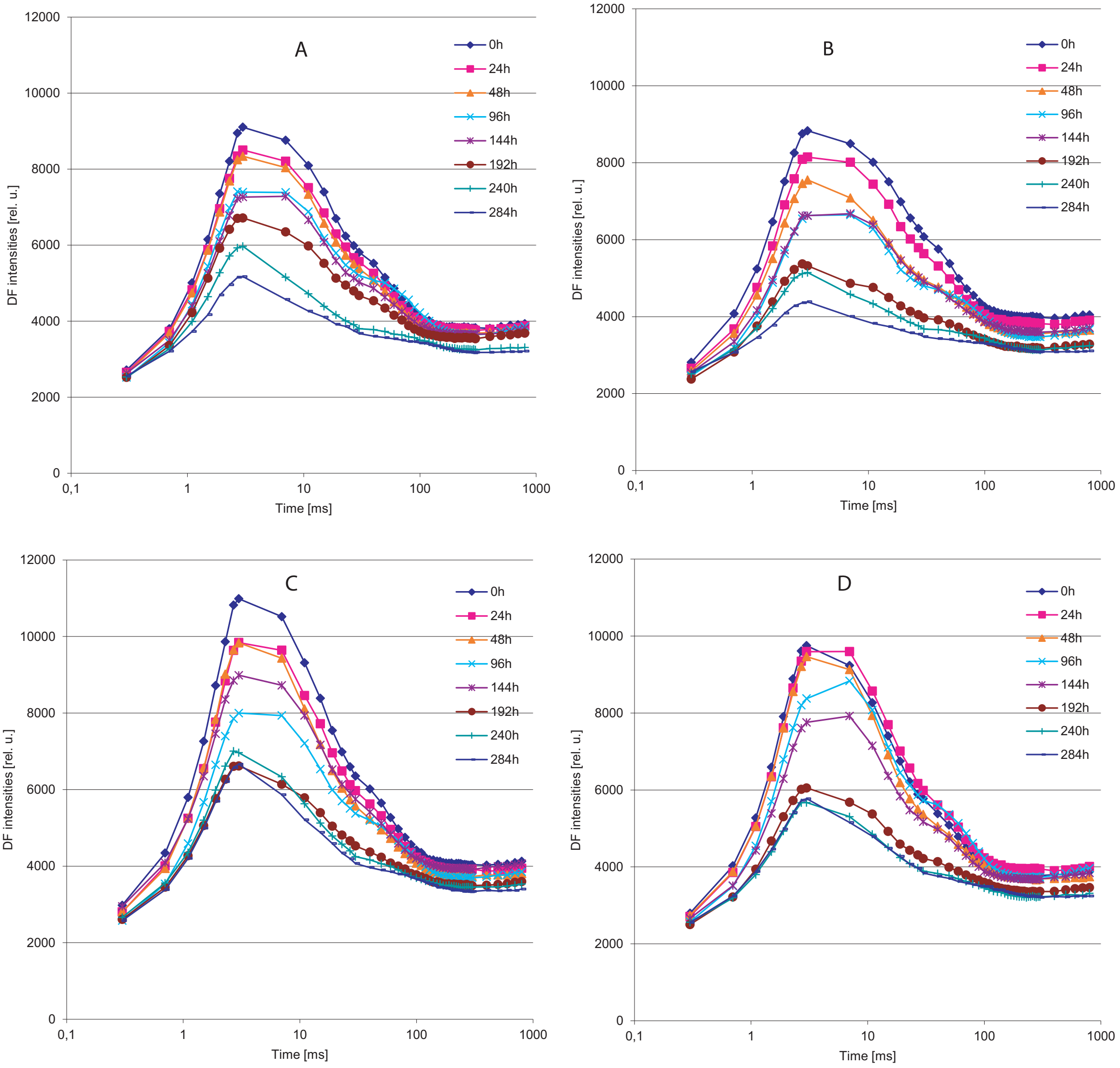

Fig. 2. Effect of the duration of the salt stress application (0 h, 24 h, 48 h, 96 h, 144 h, 192 h, 240 h and 248 h) on the delayed fluorescence induction curves in dark-adapted leaves. A: Nira treated with 0.15 M, B: Nira treated by 0.30 M salt solutions, C: Roadrunner treated with 0.15 M salt solution, D: Roadrunner treated with 0.30 M salt solution. n=9. Relative units.

decay component that occurred within a microsecond time range. In the initial part of DF induction kinetics (during the first 1 s of illumination) this emission makes a predominant contribution. The changes of the fluorescent induction curves depend on the salt solution and the perennial ryegrass variety. The curve became less visible with the passage of time exposure to stress in both varieties (Fig. 2.). However, it should be noted that in the Nira variety, growing on a saline solution at a concentration of 0.15 M caused a visible decrease in the intensity of curves measured 96 h after the application of stress. The first maximum of curve (I_1) decreased from ca. 8500 rel. u. to ca. 7000 rel. u. The curve measured 284 h after salinization had a maximum of ca. 5000 rel. u. In plants treated with a 0.30 M concentration of salt visible changes were noted 48 h after the application of stress (ca. 7500 rel. u.). In the Roadrunner variety treated with a 0.15 M concentration of salt visible changes were obtained 96 h after the application of stress (maximum declined from ca. 11000 rel. u. to ca. 8000 rel. u.) and in plants treated with a 0.30 M salt solution changes were observed 144 h after the application of stress (ca. 1000 rel. u. and ca. 8000 rel. u., respectively). 240 h after salinization the second maximum (I_2) (in the Nira variety treated with a 0.15 M salt solution) decreased significantly from ca 5600 rel. u. to ca. 4000 rel. u. In plants treated with 0.30 M changes were observed 192 h after salinization, when the maximum decreased from ca. 6000 rel. u. to ca. 4000 rel. u. In the Roadrunner variety treated with a 0.15 M solution a significant decline of the second maximum was noted 192 h after salinization (from ca. 6000 rel. u. to ca. 4000 rel. u.). In plants treated with a 0.30 M solution changes appeared 192 h after salinization as well. It should be noted that there were no differences between the minimum of the curve (D_2) measured in the control and in plants treated with salt.

To better illustrate the changed shape of the DF within the scale of time, the induction curves (IC) were calculated and averaged (Fig. 3). The ratio $(I_1–D_2)/D_2$ was changed in the Nira variety, first in those plants treated with a 0.30 M solution 192 h after salinization. After 240 h and 284 h both salt solutions caused a similar decrease in the ratio when compared with the control. In the Roadrunner variety the ratio began decrease 144 h after salinization and were similar under both salt solutions. The course of changes of ratio I_1/I_2 was the same as the changes of ratio $(I_1–D_2)/D_2$. During the induction transient (through phases I_1, I_2, D_2 etc.) the relative amplitude of the fastest component (L_1) changed.

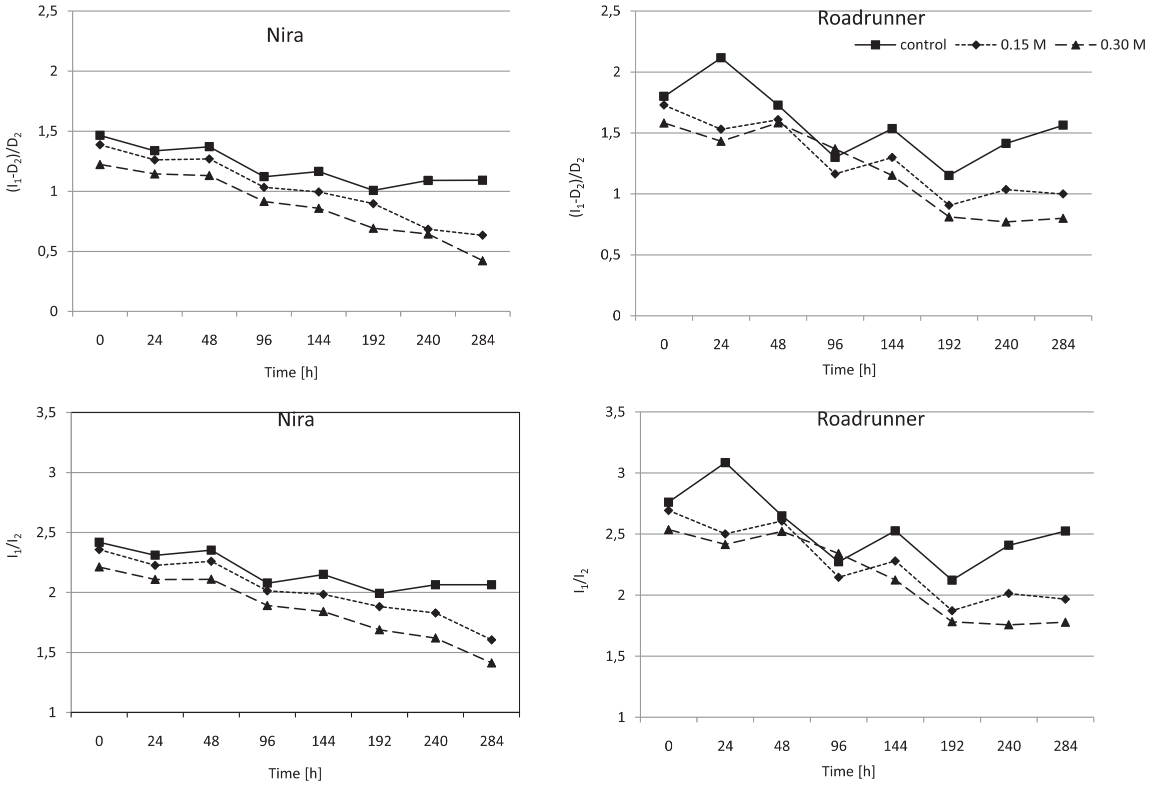

Fig. 3. The dependence of $(I_1\text{-}D_2)/D_2$ and I_1/I_2 ratios measured in leaves of Nira and Roadrunner varieties on the duration of 0 M, 0.15 M, and 0.30 M salt solution applications (0 h, 24 h, 48 h, 96 h, 144 h, 192 h, 240 h and 248 h). n=9. Relative units.

The relative contribution of this DF component at phase I_1 in the native leaves of Nira was affected by both salt solutions 192 h after stress application. I_2 phase in this variety was also affected by both salt solutions. In Roadrunner there were no significant differences between control plant and plant treated by salt. D_2 phase was no affected in both varieties (Fig. 4).

Based on the results obtained, it should be noted that the transition at 820 nm was significantly affected by salt stress in both varieties (Fig. 5). In both the Nira and Roadrunner varieties the value of the MR_{min} parameter was the lowest 96 h after the application of stress in plants treated with both salt solutions. Values measured later than 96 h were similar to the control plants and the plants under stress. The MR_{max} parameter was lower 240 h and 284 h after applying salt in plants treated with both salt solutions. Both ΔMR slow and ΔMR fast parameters in the Nira variety treated with a 0.15 M salt solution were higher 96 h after the application of stress. A similar reaction was observed in plants treated with a 0.30 M salt solution. In the Roadrunner variety the most pronounced changes were also noted 96 h after the application of stress, and they were more noticeable than in the Nira variety. The slope of the relative MR signal is shown in Fig. 6. The first parameter is the rate of initial photooxidation of P700 (V_{ox}). The second parameter is the rate of the re-reduction of $P700^+$ by electrons from PS II and the reduced PQ pool. The results showed that salt treatment does not influence the rate of P700 oxidation. There was no significant difference in parameter values between the control plants and the plants treated with salt. PS I is quite tolerant to this type of stress. The parameter V_{red} represents the process of P700+ reoxidation and reflects the electron transport rate between the photosystems. This rate was inhibited at incubation with plants having a salt solution longer than 144 h. In Nira variety treated by salt solution of 0,15 M the V_{red} parameter was decreasing in compare to control 240 h after stress application. Salt solution of 0,30 cause decreasing of this parameter 192 h after stress application. In Roadrunner variety decreasing of V_{red} parameter was caused similar by both salt solutions (0,15 and 0,30 M) 192 h after stress application.

3.2. *Gas exchange parameters*

CO_2 assimilation (*An*) was significantly influenced by salt in both varieties (Fig. 7). However, the rate of reaction depended on the variety. In Nira the significant differences between values measured in all 3 treatments were observed 48 h after salinization. The CO_2 assimilation measured in the control treatment was 3.8 μmol CO_2 m^{-2} s^{-1}, which decreased by 32% in the 0.15 M solution and by 80% in the 0.30 M solution. Later, the values of this parameter ranged from 2.3 CO_2 $m^{-2}s^{-1}$ to 2.5 CO_2 $m^{-2}s^{-1}$ under controlled conditions and were significantly greater than in 0.15 M (0.3 μmol CO_2 m^{-2} s^{-1} on average) and 0.30 M (0.2 μmol CO_2 $m^{-2}s^{-1}$ on average). There were no significant differences between the 0.15 M and 0.30 M treatments during these time frames. In Roadrunner a decrease in this parameter for the 0.15 M and 0.30 M solutions was noted 96 h after salinization. Even greater differences were noted later (144 h after salinization). Moreover, significant statistical differences between the 0.15 M and 0.30 M treatments were also found. Later significant differences between the 0.15 and 0.30 treatments with salt were hardly noted.

H_2O transpiration (*E*) in the Nira variety was affected significantly 48 h after the salt application. In the control plants this parameter was at a level of 2.4 mmol H_2O $m^{-2}s^{-1}$ and decreased to 1.6 mmol H_2O $m^{-2}s^{-1}$ in the plants treated with the 0.15 M solution, and to 1.2 mmol H_2O $m^{-2}s^{-1}$ in the plants treated with the 0.30 M solution. Significant statistical differences were noted

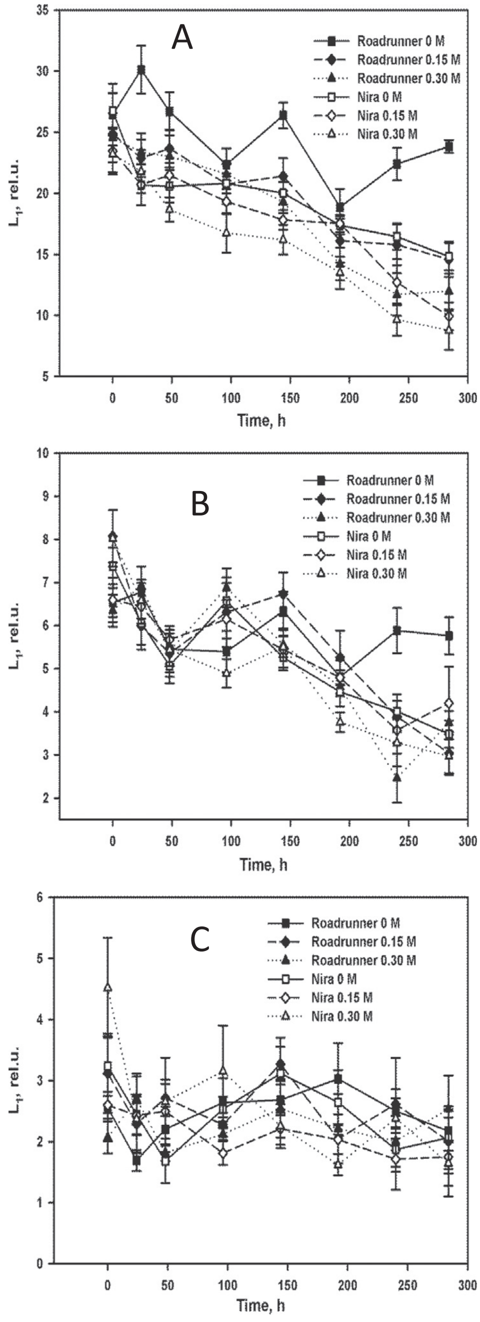

Fig. 4. The dependence of relative amplitude of the fastest component (L_1) in leaves of the Nira and Roadrunner varieties on the duration of 0 M, 0.15 M and 0.30 M salt solutions application (0 h, 24 h, 48 h, 96 h, 144 h, 192 h, 240 h and 248 h). A is for L_1 at I_1, B is for L_1 at I_2 and C is for D_2. n=9, Relative units.

only between values measured in the control and the plants treated with the 0.30 M solution. Later, significant statistical differences were noted between the control plants and the plants treated with both salt solutions, but not between those plants treated with salt solutions. In the Roadrunner variety transpiration was affected significantly 96 h after the application of stress. The value measured on the control plants was at a level of 2.8 mmol H_2O $m^{-2}s^{-1}$. Salt stress caused a decrease in the E value to 1.6 mmol H_2O $m^{-2}s^{-1}$ in the plants treated with the 0.15 M solution and to 0.7 mmol H_2O $m^{-2}s^{-1}$ in the plants treated with the 0.30 M solution. The differences were even greater 144 h after salinization. Later, there were no differences between the plants treated with the 0.15 and 0.30 M solutions. The A/E ratio was calculated based on these results. This ratio characterizes photosynthetic water-use efficiency (WUE). The ratio decreased under salt stress in both varieties, but there were no significant statistical differences between them (data not shown).

The internal CO_2 concentration (C_i) in the Nira variety was significantly affected 96 h after the application of stress. In the control plants this parameter was at the level of 448 (mmol mol^{-1} CO_2) and was higher than in the plants treated with the 0.15 M solution (351 mmol mol^{-1} CO_2) and in the plants treated with the 0.30 M solution (352 mmol mol^{-1} CO_2). Later, the values measured in the control plants were also significantly higher than in the plants treated with both salt solutions. In the Roadrunner variety significant changes were noted 192 h after the application of stress. In the control plants this parameter was on the level of 445 mmol mol^{-1} $CO_{2,}$ and decreased to 305 mmol mol^{-1} CO_2 and 370 mmol mol^{-1} CO_2 in the plants treated with salt solutions, respectively. At 192 h after salinization there were differences between the control and the plants treated with both salt solutions, but not between the salt solutions themselves.

Stomatal conductance (G_s) was significantly influenced by salt. In Nira a significant decrease was noted 96 h after salinization. The value measured in the control was 0.31 mol H_2O $m^{-2}s^{-1}$. The value measured in the plants treated with the 0.15 M solution decreased by 11%, and by 13% in the 0.30 M solution when compared with the control. The values measured in treatments with salt comprised one homogenous group. The value measured 96 h after the application of stress in the 0.15 M treatment was lower by 44% and the value measured in the 0.30 M treatment was lower by 61.3% when compared with the control. Later, the differences were even more pronounced. In Roadrunner significant differences were noted 96 h after salinization. This value decreased by 31.3% in the 0.15 M treatment and by 38.3% in the 0.30 M treatment. The value measured in the control was 0.34 mol H_2O $m^{-2}s^{-1}$144 h after the application of stress, which decreased by 44.2% in the 0.15 M treatment and by 80.1% in the 0.30 M treatment. A significance of differences between the 0.15 M and 0.30 M solutions was found. Later, the results were similar to those obtained 144 h after the application of stress.

3.3. *Relationships between DF, MR and gas exchange parameters*

Statistical analysis showed a significant correlation between some DF parameters and the gas exchange parameters (Fig. 8). In the Nira variety the *A* was significantly correlated with I_1 in the control plants (0.79) and in the plants treated with salt (0.80). The I_2 parameter in the Nira variety was correlated with *A* only in the plants treated with salt (0.77). The D_2 parameter was correlated with *An* also in the plants treated with salt (0.73). (I_1-D_2)/D_2 and I_1/I_2 ratios were correlated with *An* in the control plants and in the plants treated with salt. In the Roadrunner variety this parameter was correlated with I_1 in the control plants (0.76), as well as in the plants treated with salt (0.86). The I_2 parameter was correlated with *An* in the control plants (0.71) and in the plants treated with salt (0.73). The D_2 parameter in Roadrunner was correlated with *An* only in the plants treated with salt (0.72). The I_1-D_2/D_2 ratio was correlated in both treatments (0.73 and 0.88 respectively), but I_1/I_2 was correlated with *An* only in the plants treated with salt (0.88). Statistical analysis revealed that there were no significant correlation in the Nira variety between the *An* parameter and the MR curve parameters (Fig. 9). In the Roadrunner variety this parameter was significant and negatively correlated with the MR_0 parameter in the plants treated with salt (- 0.62). There were also significant correlations between plants treated with salt, between *An* and MRmin (0.63), and with MRmax (0.63).

An effective approach to easier analyze a big set of experimental parameters is principal component analysis (PCA) [9]. PCA evaluates variations in the values of experimental parameters and

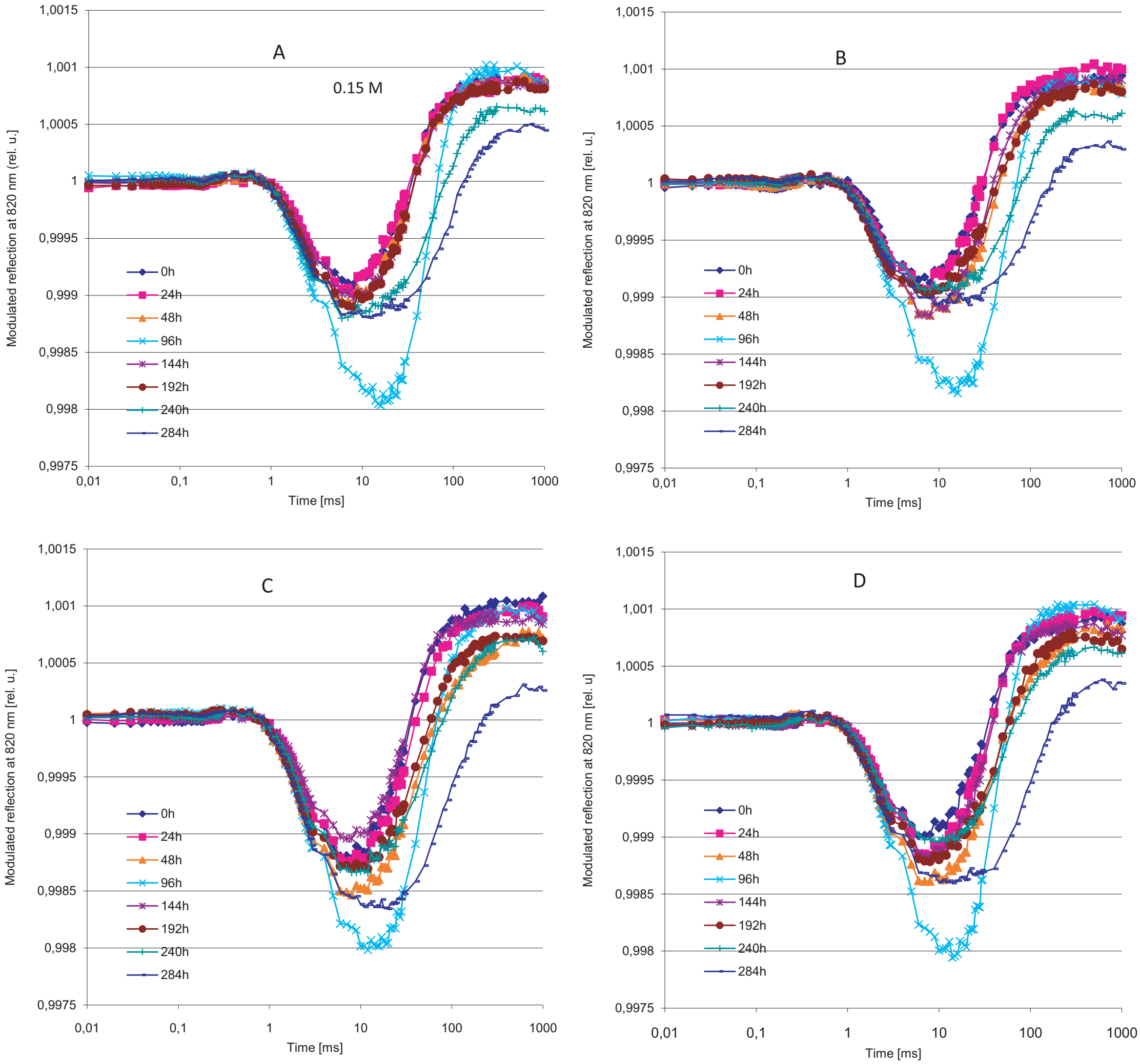

Fig. 5. Kinetics of modulated light reflection at 820 nm in dark-adapted leaves in dependence on duration (0 h, 24 h, 48 h, 96 h, 144 h, 192 h, 240 h and 248 h) of salt stress application A: Nira treated with a 0.15 M salt solution; B: Nira treated with a 0.30 M salt solution; C: Roadrunner treated with a 0.15 M salt solution; D: Roadrunner treated with a 0.30 salt solution. n=9. All data is normalized to the initial measured value of the signal. The data is presented in relative units.

derives new complex variables that reflect maximal changes in the original parameter data set. The first principal component (PC), Comp 1, is a vector in n-dimensional space (where n is a number of analyzed experimental parameters) that corresponds to maximal variations of parameters. The second PC, Comp 2 is a vector in the plane perpendicular to Comp 1 vector and reflects maximal change of parameters in the same plane.

In the vector graphs the relative “contribution” of each input variable to the formation of the principal components (Comp. 1 and Comp. 2) is presented in Fig. 10. The magnitude of the vector is an indicator of the stressor influence on the corresponding DF, MR, and gas exchange parameters. The direction of the vector is dependent upon its impact on the Component 1 and Component 2 values. In the Nira variety the modification in the first component determined about 59% of the total amount of changes and the second component determined about 16% of the total amount of changes. In the Roadrunner variety this was about 65% and 14% respectively. The parameters analyzed had different sensitivities to salt stress. In the Nira variety the formation of the first and second components stood out in relation to the changes of all the parameters except for WUE, ΔMR_{slow} and ΔMR_{fast}. In the Roadrunner variety the formation of the first component stood out in relation to the changes of MR_{min} and $\Delta MR_{fast.}$

4. Discussion

The use of the simultaneously measured DF, $MR_{820,}$ and gas exchange for monitoring the response of the photosynthetic machinery to salt stress in the two perennial ryegrass varieties had two goals: first, to examine the sensitivity at different points in the electron transport chain to salt stress, and second, to test the sensitivity of the experimental signals to changes in the status of the photosynthetic machinery during salinization. In the opinion of Lambrev and Goltsev [31], Goltsev et al. [28], or Guo and Tan [32], the high sensitivity of photosynthesis to environmental factors and the sensitivity of DF to changes in different photosynthetic processes make it a useful tool for testing plant reactions under stress conditions. Indeed, the results confirmed the significant impact of salt stress on the DF curve as well as on the gas exchange parameters.

The negative effect of salinity on the photosynthesis process has been known for a long time, but it has yet to be fully understood. The significant impact of salt on gas exchange parameters was observed by Kalaji et al. [8]. In the opinion of these authors, and also of Demming-Adams et al. [33], the reaction of photosynthesis resembles the changes occurring under photoinhibition. Results obtained by Metha et al. [34] have illustrated the gradual

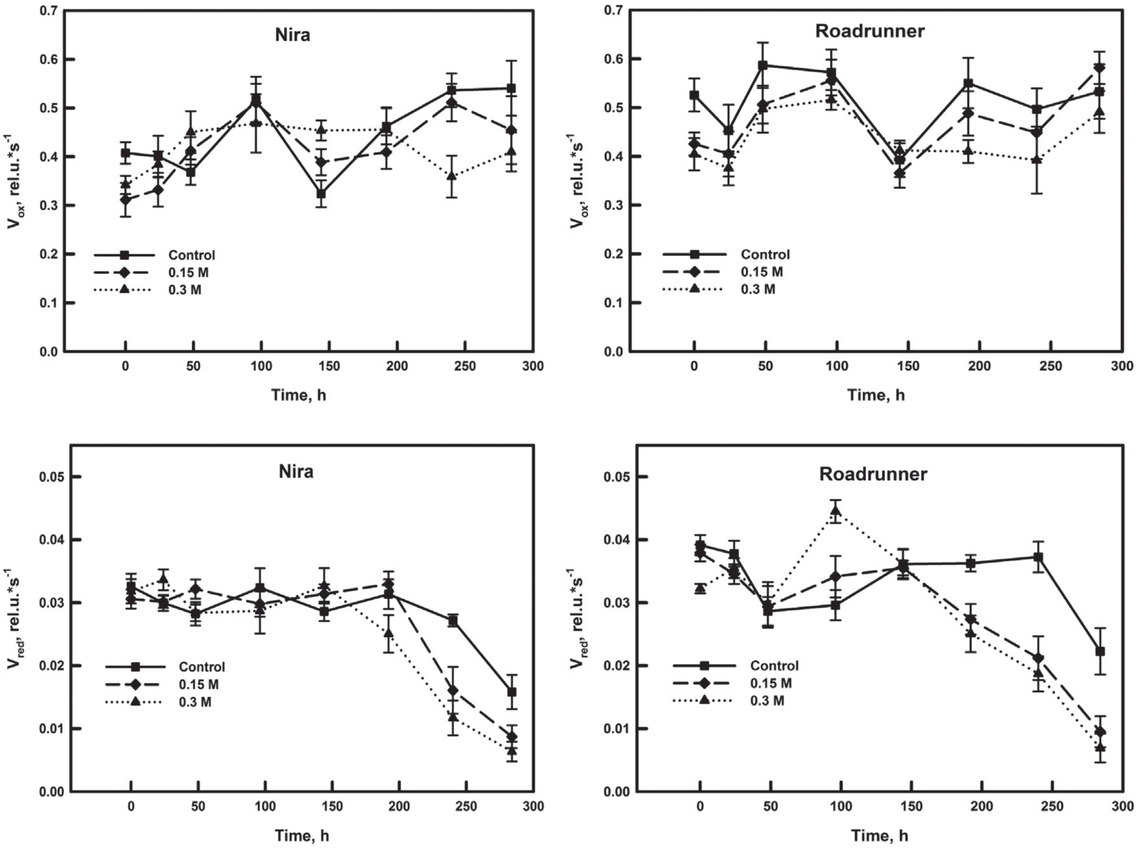

Fig. 6. The dependence of the relative rates of P700 oxidation (A and B) and P700$^+$ re-reduction (C and D) calculated from the MR820 signal measured in the leaves of Nira (A and C) and Roadrunner (B and D) varieties on the duration of 0 M, 0.15 M and 0.30 M salt solution applications (0 h, 24 h, 48 h, 96 h, 144 h, 192 h, 240 h and 248 h). n=9. Relative units.

changes in the PS II heterogeneity in plants during their development when subjected to salt stress. The initial effects of increasing soil salinity are very similar to those observed when plants are exposed to drought. A reduction in leaf water potential will reduce stomatal conductance and eventually inhibit photosynthetic metabolism [5]. The decrease in stomatal conductance under salt was also confirmed in this work. A high contamination of salt adversely affects photosynthetic efficiency both on the electron donor side or the electron acceptor side, or on both sides of PS II [34]. Under high salinity irreversible damage to the photosynthetic apparatus (associated with a reduction of ribulose-1,5-bisphosphate carboxylase/oxygenase (Rubisco) activity occurs when stress is prolonged and salt continues to accumulate in the leaves [35–38].

Allakhverdiev et al. [39] and Allakhverdiev and Murata [40] found that salt stress affected plants in terms of photosynthetic electron transport. Results obtained by Mehta et al. [41] proved that antenna size, which is further differentiated into α, β and γ PSII centers, changed under salt stress conditions. At higher salt concentrations, there was a decrease in the number of a PS II centers with a simultaneous increase in the amount of β and γ PS II centers. Oukarroum et al. [42] also confirmed that salt stress inhibited PS I and PS II activities and resulted in a decrease in the overall activity of the electron transport chain while stimulating ROS (reactive oxygen species) production. The reduced electron transport chain efficiency resulted from the loss of PS II activity and the damage to PS I function provides a reasonable explanation for the significant changes of the $(I_1\text{-}D_2)/D_2$ ratio. In the opinion of Lazár [43] and Metha et al. [41], the $I_1\text{-}D_2/D_2$ parameter reflects the rate of electron transport in the PS II acceptor side, which is dependent upon the redox state of Q_A, Q_B, and the PQ pool. Our results confirm that the $(I_1\text{-}D_2)/D_2$ parameter was significantly affected by salt in both varieties. However, in the Nira variety changes of this ratio were visible. The formation of the first maximum (I_1) can be related to two types of phenomena. First is the photochemical-accumulation of certain redox states that are capable of charge recombination and of DF light quanta emission (these states are known as "light-emitting"). Second is the non-photochemical-amplification of DF by the electrical gradient formed by PS I [27,43]. Our results proved that the I_1 parameter was significantly influenced by salt stress in both varieties, though, in Nira, the changes were more pronounced. The I_2 maximum is usually observed with the reduction of the PQ pool and, consequentially, when the disappearance of P700$^+$ and the decrease of the transmembrane electrical gradient begin [26]. Goltsev et al. [27] suggested that I_2 was connected to the dynamics of the concentration of the light-emitting states of the PS II reaction center, when the electron transfer from Q_B to PQ starts, rather than with the presence of the transmembrane electrical gradient. The I_2 parameter was significantly affected by salt in both varieties, but in the Nira variety the changes were more pronounced. With our results, the changes in one more characteristic point, D_2, was observed. This minimum coincides with the maximal concentration of reduced P700. The PQ pool is reduced and the acceptor side of PS I is still inactive [27]. It must be noted, that the sensitivity of each DF parameter to photosynthesis was dependent upon the variety. In the Nira variety *An* was in correlation with all DF parameters except for D_2, *E* was in correlation with all DF parameters except for I_2, G_s was not in correlation only with I_1/I_2, C_i was not in correlation with any DF parameters and WUE was in correlation with $I_1\text{-}D_2/D_2$ and to I_1/I_2 (data not shown). In Roadrunner, generally, correlations were more pronounced when

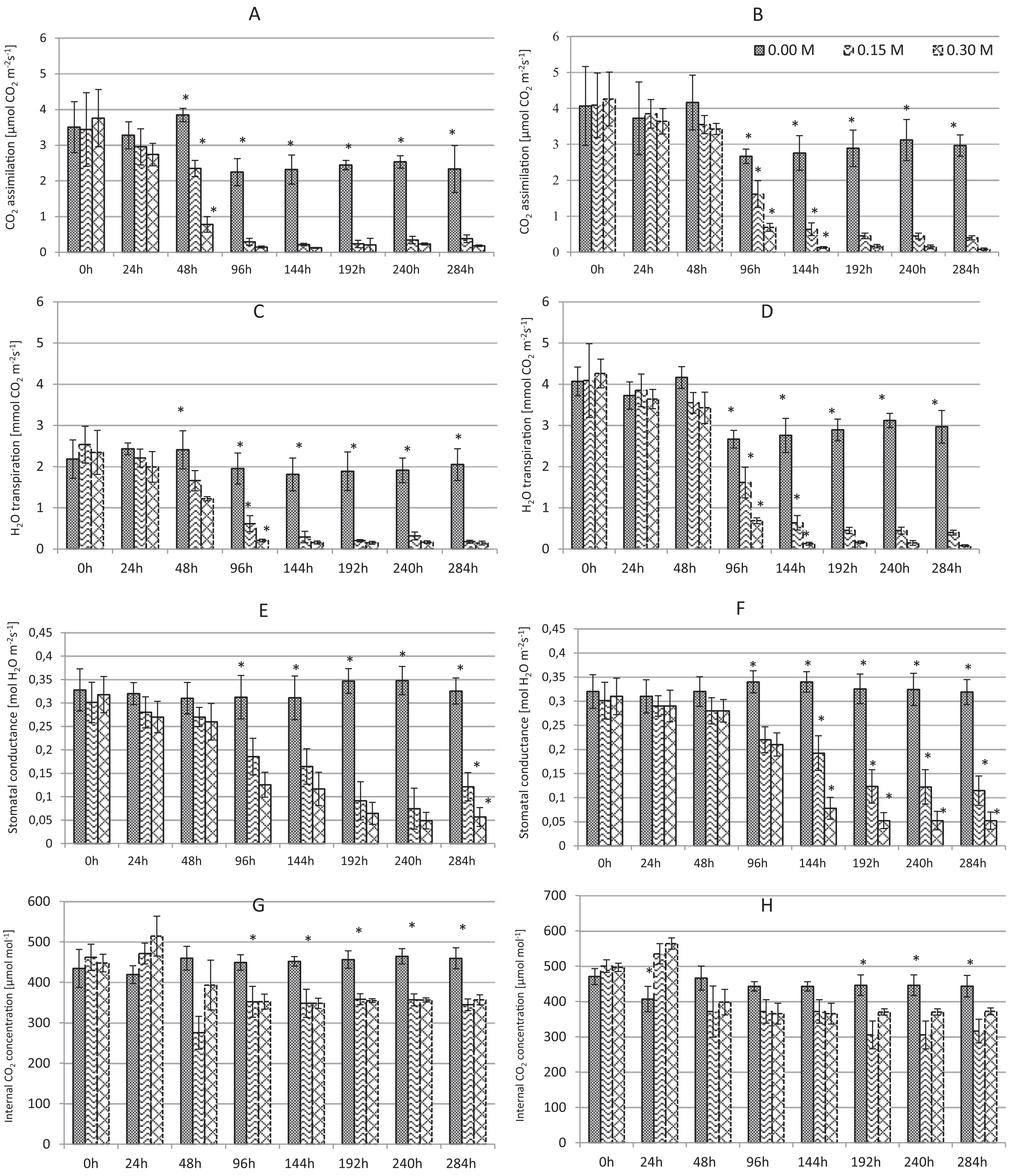

Fig. 7. The dependence of gas exchange parameters of the Nira and Roadrunner varieties treated with 0 M, 0.15 M and 0.30 M salt solutions at different times after the application of stress (0 h, 24 h, 48 h, 96 h, 144 h, 192 h, 240 h and 248 h). A: CO_2 assimilation (*An*) in Nira; B: CO_2 assimilation (*An*) in Roadrunner; C: H_2O transpiration (*E*) in Nira, D: H_2O transpiration (*E*) in Roadrunner, E: stomatal conductance (g_s) in Nira, F: stomatal conductance (G_s) in Roadrunner, G: internal CO_2 concentration (C_i) in Nira, H: internal CO_2 concentration (C_i) in Roadrunner. The standard deviation bars are shown. The means significant different within one variety and time frame are marked with an asterisk and differ significantly ($p < 0.05$, $n = 9$).

compared with Nira. *An* was in correlation with all DF parameters, as well as with *E* and G_s. $C_i$parameters were not in correlation with any DF parameters.

We have observed a significant decrease in the minimum of the MR signal under salt stress condition in both varieties (Figs. 5 and 6). In the opinion of many authors [29,44,45], the MR signal is mainly affected by the rate of electron flow from PS II to PS I. Salt induced modification of the Q_B binding site on the D1 protein of PS II could cause a block on the electron transfer from PS II to cyt b_6f and to PS I consequently. Moreover, the limitation on the acceptor side of PS I was also probably the reason for the changing MR signal [46]. Our results suggest that there were no significant differences between the values of the ΔMR_{slow} and ΔMR_{fast} parameters (observed as the differences between MR_{max} and MR_{min} and between MR_0 and MR_{min}) measured in the control plants and in the plants treated with salt. Moreover, there was no correlation between these parameters and the gas exchange parameters. These results are in discrepancy with other authors, who suggested that these parameters were sensitive to stress. Schansker and co-authors [29] suggested that the fast phase of the signal corresponds to the kinetics of the photoinduced changes in the P700 redox state, being significantly modified only by strong stress, but the slow phase of the MR signal, reflecting a $P700^+$ re-reduction, was more sensitive and decreased progressively with

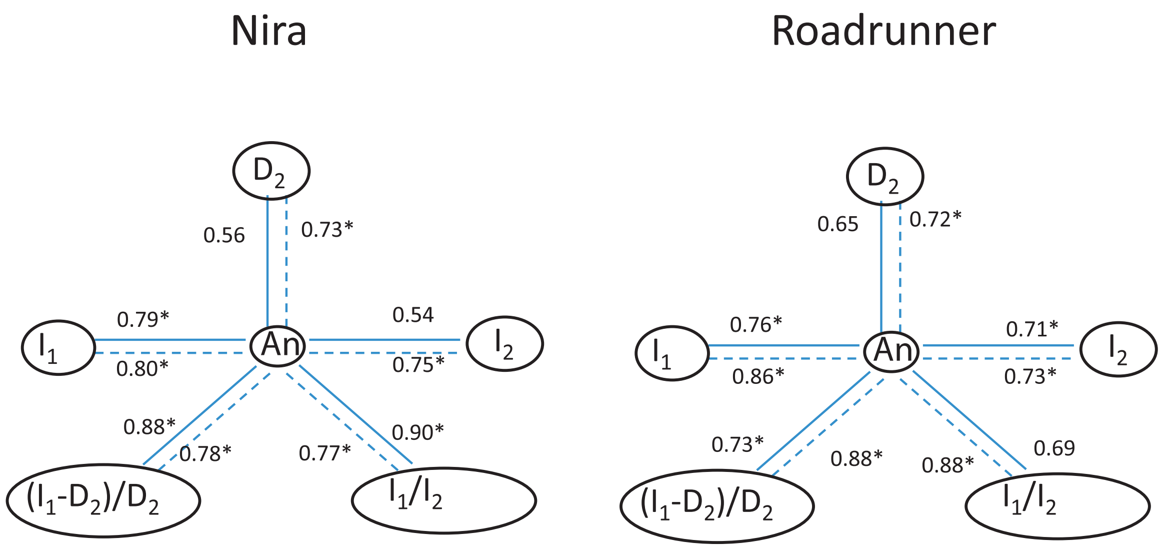

Fig. 8. Correlation coefficients (*r*) between delayed fluorescence parameters and gas exchange parameters (correlations significant at $p < 0.05$). *An* – CO_2 assimilation, E - H_2O transpiration, G_s - stomatal conductance, C_i - internal CO_2 concentration.

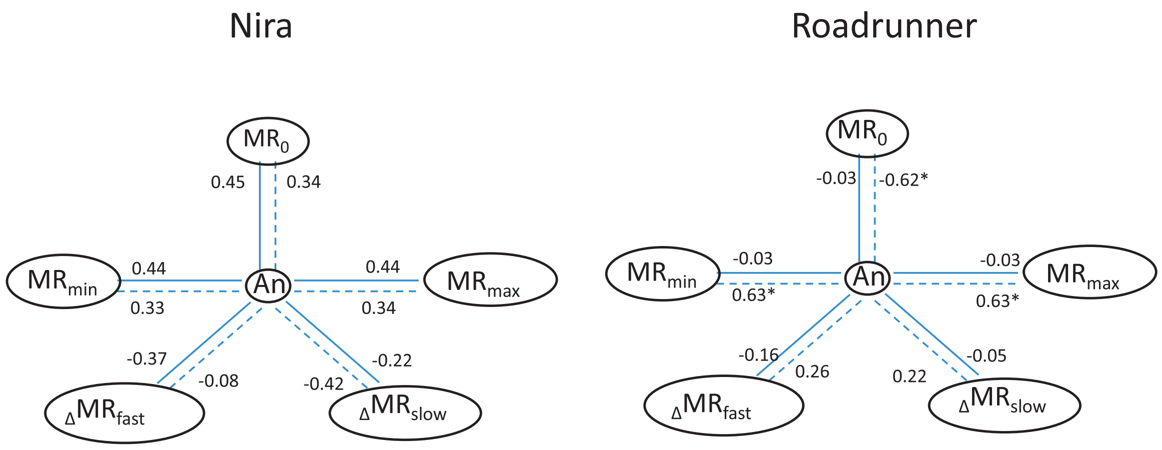

Fig. 9. Correlation coefficients (*r*) between modulated reflection at 820 nm parameters and gas exchange parameters (correlations significant at $p < 0.05$). *An* – CO_2 assimilation, E - H_2O transpiration, G_s - stomatal conductance, C_i - internal CO_2 concentration.

stress intensity. Probably, the deactivation of this kinetic phase is manifested as a diminished rate of electron transport through plastoquinone to $P700^+$, and is the reason for the more stable fast phase of the MR signal [47,48].

It is essential to recognize that the main advantage of this analysis is that it is quick, and is based on measurements by a non-invasive and a highly sensitive and accurate method. However, simultaneously measurements with other methods are necessary to obtain a complete picture. Because of this reason, measurements on photosynthesis (CO_2 assimilation) was included in this work. Salt effects on gas exchange processes fall into two major categories. The first is the response of stomates to salinization of the plant. The second is the effects of salt on the capacity of the plant for CO_2 fixation, independent of altered diffusion limitations. Stomatal closure is generally associated with salinization of salt-sensitive species [8]. The data presented by these authors for barley indicate that stomatal conductance is reduced by salinity. However, the extent to which stomatal closure affects photosynthetic capacity is indicated by the magnitude of the reduction in *Ci*. The salt-induced decline in *Ci*.

The measurements of DF and MR820 can be used to effectively describing the electron transport of PSII. Delayed fluorescence data gave additional information about the change in the antenna size heterogeneity of PSII. From this work, we conclude that DF and MR820, both measured together, can give reliable information on structural and functional changes occurring at PSII under salt stress condition. Their simultaneous recording, with one instrument does not simply facilitate the collection of information. As shown in this work, the main advantages, related also with the high time resolution of M-PEA, are the collection of a lot of information, more than by the separate recordings so far.

5. Conclusions

The DF curve is complex and multi-component. Several components take part in its formation, and each component depends in a different way on the reactions of electron transfer in the PS II acceptor side and on thylakoid membrane energization. The evaluation of the contribution and of the properties of each of the components can transform the DF into an information-rich quantitative method for the analysis of photosynthetic reactions in vivo. Our experiments allowed us to determine how delayed chlorophyll *a* fluorescence parameters were most significantly altered under salinity stress (all of the parameters from DF curve analyzed were affected, except for D_2). From these results we also conclude that an increase in salt concentration influences the activity of PS II. There are significant differences between the perennial ryegrass lawn

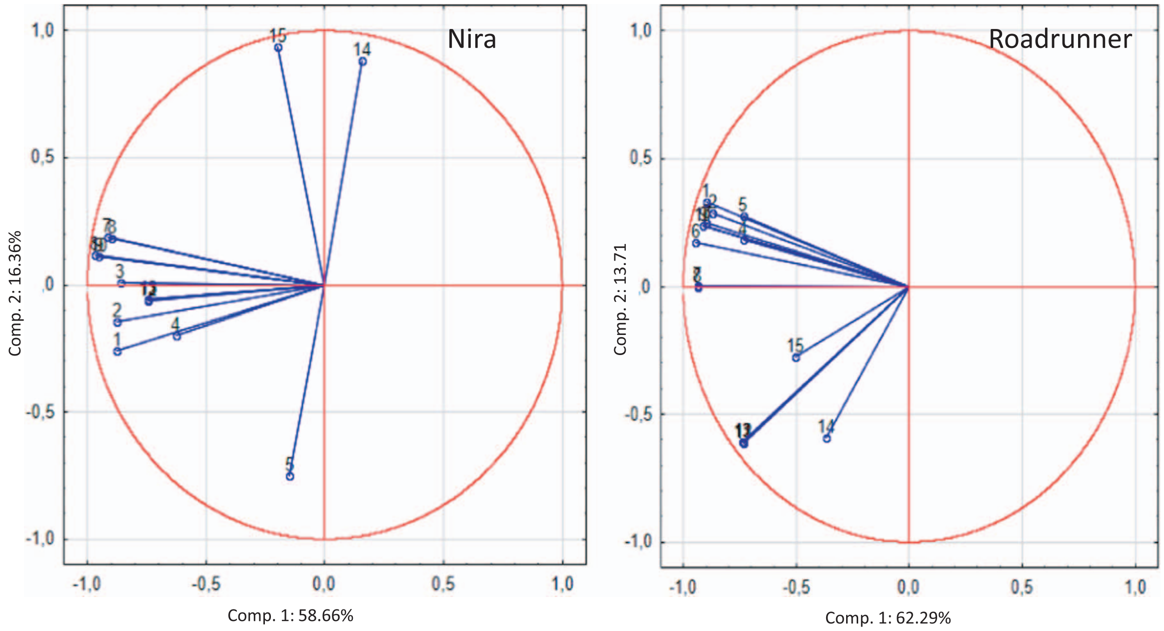

Fig. 10. Vector graphs showing the relative "contribution" of each input to the formation of the principal components. 1: *An*; 2: *E*; 3: G_s; 4; C_i; 5: WUE; 6: I_1; 7: I_2; 8: D_2; 9: $(I_1\text{-}D_2)/D_2$; 10: I_1/I_2; 11: MR_0; 12: MR_{min}; 13: MR_{max}; 14: $_{\Delta}MR_{fast}$; 15; $_{\Delta}MR_{slow}$.

varieties tested in terms of their adaptation to NaCl stress. This knowledge can lead to the selection of plants with a higher potential for photosynthetic efficiency (vitality) under conditions of salt stress, which can be used successfully on neighboring roads where salt is applied. Very different responses to NaCl stress in the two perennial ryegrass lawn varieties were observed.

Authors' contributions

P. Dąbrowski and M.H. Kalaji designed the study. P. Dabrowski, A.H. Baczewska and P. Pawluśkiewicz conduced the experiment. M. Paunov and V. Goltsev performed the statistical analysis. G. Mastalerczuk and B. Borawska – Jarmułowicz did editing the manuscript. Author contributions in percentage: P. Dabrowski 50%, H.M. Kalaji 10%, A.H. Baczewska 10%, B. Pawluśkiewicz 5%, G. Mastalerczuk 5%, Barbara Borawska – Jarmułowicz 5%, V. Goltsev 10% and M. Paunov 5%.

Formatting of funding sources

This work was funded by the Rector of the Warsaw University of Life Sciences (SGGW).

References

[1] P. Dąbrowski, B. Pawluśkiewicz, H.M. Kalaji, A.H. Baczewska, The effect of light availability on leaf area index, biomass production and plant species composition of park grasslands in Warsaw, Plant Soil Environ. 59 (2013) 543–548.
[2] X. Ma, J. Zhang, B. Huang, Cytokinin-mitigation of salt-induced leaf senescence in perennial ryegrass involving the activation of antioxidant systems and ionic balance, Environ. Exp. Bot. 125 (2016) 1–11.
[3] A.H. Baczewska, W. Dmuchowski, A. Jozwiak, D. Gozdowski, P. Brągoszewska, P. Dąbrowski, E. Swiezewska, Effect of salt stress on prenol lipids in the leaves of Tilia 'Euchlora', Dendrobiology 72 (2014) 177–186.
[4] K. Maxwell, G.N. Johnson, Chlorophyll fluorescence: a practical guide, J. Exp. Bot. 51 (2000) 659–668.
[5] N.R. Baker, E. Rosenqvist, Applications of chlorophyll fluorescence can improve crop production strategies: an examination of future possibilities, J. Exp. Bot. 55 (2004) 1607–1621.
[6] P. Dąbrowski, A.H. Baczewska, B. Pawluśkiewicz, M. Paunov, V. Goltsev, M. H. Kalaji, Prompt chlorophyll a fluorescence as a rapid tool for diagnostic changes in PS II structure inhibited by salt stress in perennial ryegrass, J. Photochem. Photobiol. B-Biol. 157 (2016) 22–31.
[7] P. Dąbrowski, B. Pawluśkiewicz, A.H. Baczewska, I. Łukasik, V. Goltsev, H.M. Kalaji, Evaluation the vigour of urban green lawn grown under long-term shade conditions by the use of chlorophyll fluorescence technique, Ann. Wars. Univ. Life Sci. SGGW 47 (2015) 203–210, Land Reclamation.
[8] H.M. Kalaji, K. Bosa, J. Kościelniak, K. Żuk-Gołaszewska, Effects of salt stress on photosystem II efficiency and CO2 assimilation of two syrian barley landraces, Environ. Exp. Bot. 73 (2011) 64–72.
[9] H.M. Kalaji, M.D. Cetner, I.A. Samborska, A. Oukarroum, S. Rusinkowski, S. Pietkiewicz, M. Świątek, P. Dąbrowski, Effective microorganisms impact on photosynthetic activity of arabidopsis plant grown under salinity stress conditions, Ann. Wars. Univ. Life Sci. SGGW 48 (2016) 153–163, Land Reclamation.
[10] P. Dąbrowski, B. Pawluśkiewicz, A.H. Baczewska, P. Oglęcki, H.M. Kalaji, Chlorophyll a fluorescence of perennial ryegrass (Lolium perenne L.) varieties under long term exposure to shade, Zemdirb. Agric. 102 (2015) 305–312.
[11] Č.N. Radenović, G.V. Maksimov, E.V. Tyutyaev, G.J. Stanković, Ž.V. Jovanović, M.V. Beljanski, Detecting the phase transition in thylakoid membranes of maize in bred lines by means of delayed fluorescence, Plant Physiol. Biochem. 81 (2014) 208–211.
[12] V. Goltsev, I. Zaharieva, P. Lambrev, I. Yordanov, R. Strasser, Simultaneous analysis of prompt and delayed chlorophyll a fluorescence in leaves during the induction period of dark to light adaptation, J. Theor. Biol. 225 (2003) 171–183.
[13] H.M. Kalaji, A. Jajoo, A. Oukarroum, M. Brestic, M. Zivcak, I.A. Samborska, M. D. Cetner, I. Łukasik, V. Goltsev, R.J. Ladle, Chlorophyll a fluorescence as a tool to monitor physiological status of plants under abiotic stress conditions, Acta Physiol. Plant. 38 (2016) 102.
[14] M. Havaux, Rapid photosynthetic adaptation to heat stress triggered in potato leaves by moderately elevated temperatures, Plant Cell Environ. 16 (2016) (1993) 461–467.
[15] Y. He, Z. Zhu, J. Yang, X. Ni, B. Zhu, Grafting increases the salt tolerance of tomato by improvement of photosynthesis and enhancement of antioxidant enzymes activity, Environ. Exp. Bot. 66 (2009) 270–278.
[16] R. Zhang, T.D. Sharkey, Photosynthetic electron transport and proton flux under moderate heat stress, Photosynth. Res. 100 (2009) (2009) 29–43.
[17] P. Mehta, A. Jajoo, S. Mathur, S. Bharti, Chlorophyll a fluorescence study revealing effects of high salt stress on photosystem II in wheat leaves, Plant Physiol. Biochem. 48 (2010) 16–20.
[18] R. Singh-Tomar, S. Mathur, S.I. Allakhverdiev, A. Jajoo, Changes in PSII heterogeneity in response to osmotic and ionic stress in wheat leaves (Triticum aestivum), J. Bioenerg. Biomembr. 44 (2012) 411–419.
[19] Y. Guo, J. Tan, Fourier transform of delayed fluorescence as an indicator of herbicide concentration, J. Theor. Biol. 363 (2014) (2014) 271–276.
[20] A. Oukarroum, V. Goltsev, R.J. Strasser, Temperature effects on pea plants probed by simultaneous measurements of the kinetics of prompt fluorescence, delayed fluorescence and modulated 820 nm reflection, PLoS ONE 8 (2013) e59433.
[21] Y. Guo, J. Tan, Applications of delayed fluorescence from photosystem II, Sensors 13 (2013) 17332–17345.
[22] V. Goltsev, I. Zaharieva, P. Chernev, R. Strasser, Delayed chlorophyll fluorescence as a monitor for physiological state of photosynthetic apparatus,

Biotechnol. Biotechnol. Equip. 23 (2009) 452–457.
[23] A. Scordino, A. Triglia, F. Musumeci, Analogous features of delayed luminescence from acetabularia acetabulum and some solid state systems, J. Photochem. Photobiol. B: Biol. 56 (2000) 181–186.
[24] W.T. Stacy, T. Mar, C.E. Swenberg, An analysis of a triplet exciton model for the delayed light in chlorella, Photochem. Photobiol. 14 (1971) 197–219.
[25] F. Rappaport, M. Guergova-Kuras, P.J. Nixon, B.A. Diner, J. Lavergne, Kinetic and pathways of charge recombination in photosystem II, Biochemistry 41 (2002) 8518–8527.
[26] I. Zaharieva, V. Goltsev, Advances on photosystem II investigation by measurement of delayed chlorophyll fluorescence by a phosphoroscopic method, Photochem. Photobiol. 77 (2003) 292–298.
[27] V. Goltsev, P. Chernev, I. Zaharieva, P. Lambrev, R. Strasser, Kinetics of delayed chlorophyll a fluorescence registered in milliseconds time range, Photosynth. Res. 84 (2005) (2005) 209–215.
[28] V. Goltsev, I. Zaharieva, P. Chernev, R. Strasser, Delayed fluorescence in photosynthesis, Photosynth. Res. 101 (2009) 217–232.
[29] G. Schansker, A. Srivastava, Govindjee, R.J. Strasser, Characterization of the 820-nm transmission signal paralleling the chlorophyll a fluorescence rise (OJIP) in pea leaves, Funct. Plant Biol. 30 (2003) 785–796.
[30] R.J. Strasser, M. Tsimilli-Michael, S. Qiang, V. Goltsev, Simultaneous in vivo recording of prompt and delayed fluorescence and 820 nm reflection changes during drying and after rehydration of the resurrection plant Haberlea rhodopensis, Biochim. Biophys. Acta Bioenerg. 2010 (1797) 1313–1326.
[31] P. Lambrev, V. Goltsev, pH dependence of the effects of diuron, atrazine and dinoseb on the luminescent properties of thylakoid membranes, Bulg. J. Plant Physiol. 27 (2001) 85–100.
[32] Y. Guo, J. Tan, A kinetic model structure for delayed fluorescence from plants, BioSystems 95 (2009) 98–103.
[33] B. Demmig-Adams, W.W. Adams III, A. Mattoo, Photoprotection, photoinhibition, gene regulation, and environment, in: Govindjee (Ed.), Advances in Photosynthesis and Respiration, 21, Springer, Dordrecht, 2005 (reprinted 2008).
[34] P. Mehta, S.I. Allakhverdiev, A. Jajoo, Characterization of photosystem II heterogeneity in response to high salt stress in wheat leaves (Triticum aestivum), Photosynth. Res. 105 (2010) 249–255.
[35] P. Mehta, A. Jajoo, S. Mathur, S. Bharti, Chlorophyll a fluorescence study revealing effects of high salt stress on PS II in wheat leaves, Plant Physiol. Biochem. 48 (2010) 16–20.
[36] H.-W. Koyro, T. Hussaina, B. Huchzermeyerc, M.A. Khan, Photosynthetic and growth responses of a perennial halophytic grass panicum turgidum to increasing NaCl concentrations, Environ. Exp. Bot. 91 (2013) 22–29.
[37] M.E. Farias, E.G. Martinazzo, M.A. Bacarin, Chlorophyll fluorescence in the evaluation of photosynthetic electron transport chain inhibitors in the pea, Rev. Ciênc. Agron. 47 (2016) 178–186.
[38] E.N. Silva, R.V. Ribeiro, S.L. Ferreira-Silva, R.A. Viégas, J.A.G. Silveira, Comparative effects of salinity and water stress on photosynthesis, water relations and growth of Jatropha curcas plants, J. Arid Environ. 74 (2010) 1130–1137.
[39] S.I. Allakhverdiev, Y. Nishiyama, S. Miyairi, H. Yamamoto, N. Inagaki, Y. Kanesaki, N. Murata, Salt stress inhibits the repair of photodamaged photosystem II by suppressing the transcription and translation of psbA genes in *Synechocystis*, Plant Physiol. 130 (2002) 1443–1453.
[40] S.I. Allakhverdiev, N. Murata, Environmental stress inhibits the synthesis de novo of proteins involved in the photodamage-repair cycle of photosystem II in *Synechocystis* sp. PCC 6803, Biochim. Biophys. Acta 2004 (1657) 23–32.
[41] P. Mehta, V. Kraslavsky, S. Bharti, S.I. Allakhverdiev, A. Jajoo, Analysis of salt stress induced changes in photosystem II heterogeneity by prompt fluorescence and delayed fluorescence in wheat (Triticum aestivum) leaves, J. Photochem. Photobiol. B: Biol. 104 (2011) 308–313.
[42] A. Oukarroum, F. Bussotti, V. Goltsev, H.M. Kalaji, Correlation between reactive oxygen species production and photochemistry of photosystems I and II in Lemna gibba L. plants under salt stress, Environ. Exp. Bot. 109 (2015) 80–88.
[43] D. Lazár, Chlorophyll a fluorescence induction, Biochim. Biophys. Acta 1412 (1999) 1–28.
[44] P.D. Gould, P. Diaz, C. Hogben, J. Kusakina, R. Salem, J. Hartwell, A. Hall, Delayed fluorescence as a universal tool for the measurement of circadian rhythms in higher plants, Plant J. 58 (2009) 893–901.
[45] S. Hamdani, M. Qu, C.-P. Xin, M. Li, C. Chu, Govindjee, X.-G. Zhu, Variations between the photosynthetic properties of elite and landrace chinese rice cultivars revealed by simultaneous measurements of 820 nm transmission signal and chlorophyll a fluorescence induction, J. Plant Physiol. 177 (2015) 128–138.
[46] D. Lazar, Modelling of light-induced chlorophyll a fluorescence rise (O–J–I–P transient) and changes in 820 nm-transmittance signal of photosynthesis, Photosynthetica 47 (2009) 483–498.
[47] V. Goltsev, I. Zaharieva, P. Chernev, M. Kouzmanova, H.M. Kalaji, I. Yordanov, V. Krasteva, V. Alexandrov, D. Stefanov, S.I. Allakhverdiev, R.J. Strasser, Drought-induced modifications of photosynthetic electron transport in intact leaves: analysis and use of neural networks as a tool for a rapid non-invasive estimation, Biochim. Biophys. Acta 1817 (2012) 1490–1498.
[48] E. Salvatori, L. Fusaro, E. Gottardini, M. Pollastrini, V. Goltsev, R.J. Strasser, F. Bussotti, Plant stress analysis: application of prompt, delayed chlorophyll fluorescence and 820 nm modulated reflectance. Insights from independent experiments, Plant Physiol. Biochem. 85 (2014) 105–113.